Cancer vaccine strategies to improve immunotherapy: many roads lead to Rome
Tondini, E.

Citation
Tondini, E. (2021, October 21). *Cancer vaccine strategies to improve immunotherapy: many roads lead to Rome*. Retrieved from https://hdl.handle.net/1887/3217801

CATIONIC SYNTHETIC LONG PEPTIDES-LOADED NANOGELS: AN EFFICIENT THERAPEUTIC VACCINE FORMULATION FOR INDUCTION OF T-CELL RESPONSES

6

Kordalivand N*, Tondini E*, Lau CYJ, Vermonden T, Mastrobattista E, Hennink WE, Ossendorp F, Nostrum CFV

*equal contribution

ABSTRACT

Recent studies have shown a high potency of protein-based vaccines for cell-mediated cancer immunotherapy. However, due to their poor cellular uptake, efficient immune responses with soluble protein antigens are often not observed. As a result of superior cellular uptake, nanogels loaded with antigenic peptides were investigated in this study as carrier systems for cancer immunotherapy. Different synthetic long peptides (SLPs) containing the CTL and CD4+ T-helper (Help) epitopes were synthesized and covalently conjugated via disulfide bonds to the polymeric network of cationic dextran nanogels. Cationic nanogels with a size of 210 nm, positive zeta potential (+24 mV) and high peptide loading content (15%) showed triggered release of the loaded peptides under reducing conditions. An *in vitro* study demonstrated the capability of cationic nanogels to mature dendritic cells (DCs). Importantly, covalently SLP-loaded nanogels adjuvanted with poly(I:C) showed superior CD8+ T cell responses compared to soluble peptides and nanogel formulations with physically loaded peptides both *in vitro* and *in vivo*. In conclusion, covalently SLPs-loaded cationic nanogels are a promising system to provoke immune responses for therapeutic cancer vaccination.
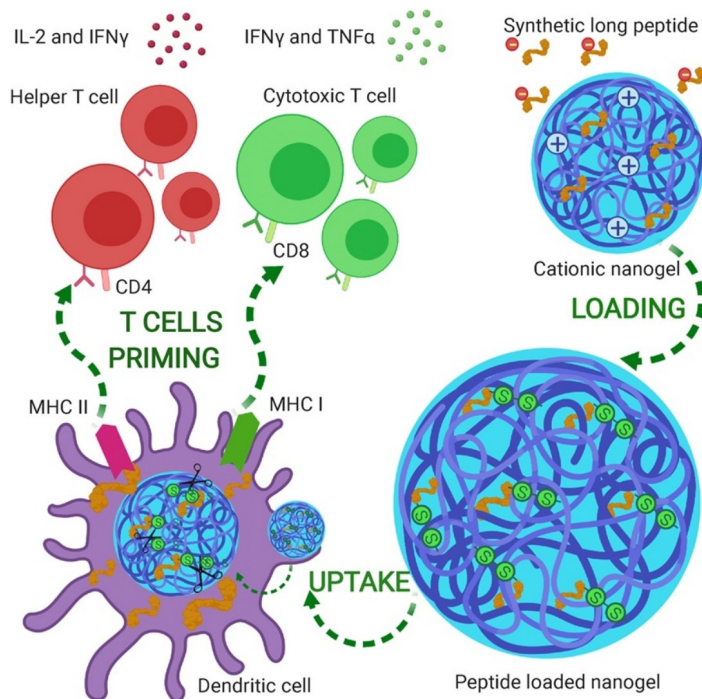
INTRODUCTION

Therapeutic vaccination has attracted much attention in recent years as a promising strategy for the treatment of different types of cancers. Stimulation of CD8$^+$ cytotoxic T lymphocytes (CTLs) and CD4$^+$ T- helper (Th) cells through MHC class I and class II pathways, respectively, is fundamental to induce effective antitumor responses [1-3]. Dendritic cells (DCs) as the most specialized antigen-presenting cells (APCs) play a crucial role in the activation of T-cell immune responses and subsequent tumor eradication [4-8]. Synthetic long peptides (SLPs) including CTL and Th epitopes were successful in clinical trials against several tumor types due to their remarkable ability to elicit a cellular immune response [9-11]. Despite superior characteristics compared to protein-based vaccines [12-13], SLPs have also important drawbacks including their susceptibility for enzymatic degradation, rapid clearance from the injection site and poor cellular uptake that limit their therapeutic efficacy [9-10, 14-15].

Different vehicles have been developed to formulate SLPs as well as other soluble antigens with the aim to improve their therapeutic effects [16-22]. Montanide, a water-in-oil emulsion-based vaccine formulation has been extensively used in clinical trials to deliver SLPs into DCs [23-25]. In 2011, a phase III clinical trial was conducted in patients with advanced melanoma. Three subcutaneous injections at 3 week intervals of Montanide-based vaccine (gp100209-217) showed significant improvement in response rates and progression-free survival compared to interleukin-2 treatment alone [26]. Oka et al. showed strong induction of antigen-specific CD8$^+$ CTL responses in patients immunized with WT-1-derived peptide vaccine in Montanide [27]. However, it was shown that due to T cell dysfunction and deletion resulting from the depot at the injection site, complete tumor eradication did not occur[28]. Therefore, due to the drawbacks of these emulsion formulations such as local adverse side effects at the site of injection, poor stability and non-controlled release kinetics, alternative delivery methods like particulate delivery systems have recently gained growing interest [29-31]. Self-assembling peptide-based systems are an alternative approach to enhance the cellular uptake of peptides and raise immunogenicity against peptide epitope vaccines [32]. Black et al. showed that self-assembled diC16-OVA provide effective *in vivo* protection from tumors by stimulating OVA-specific T-cells. By anchoring the hydrophobic tail into cell membranes, these nano-sized micelles improve the DCs uptake without TLR stimulation [33].

Moreover, it has been demonstrated that poly(lactic-*co*-glycolic acid) (PLGA)

nanoparticles can be used to encapsulate SLPs and provoke T-cell responses. By optimizing these nanoparticles regarding loading and release as well as size, Silva *et al.* showed an enhanced CD8+ T cell activation in vitro when compared to soluble peptides [34]. Hamdy et al. showed effective activation of T cells and induction of therapeutic antitumor effects in B16 melanoma tumors by co-encapsulating of TRP2$_{180-188}$ along with TLR ligand A into PLGA nanoparticles [35]. L-BLP25, a liposome-based vaccine showed strong survival rates in phase I and II trials in non-small cell lung cancer patients [36]. In a recent *in vivo* study, Varypataki *et al.* showed a remarkable capacity of cationic liposome formulation as an antigen delivery system [31] indicating that particulate systems are attractive candidates as SLP delivery platforms with clinical translation potential.

Among various nanoparticulate systems, nanogels have shown excellent properties as systems for the intracellular delivery of biopharmaceuticals including therapeutic antigens [38-42]. These nano-sized crosslinked networks are able to load biopharmaceuticals such as proteins and peptides and to protect them against undesirable (enzymatic) degradation [43-45]. Their properties can be tailored by varying the particle size, cross-link density and surface chemistry (PEGylation and targeting ligand decorations) [46-48]. The particle size and surface chemistry of nanogels largely influence their internalization by different cells. It has been shown that the uptake of relatively large particle (>1 µm) occurs by phagocytosis, whereas particles with a size between 500 nm - 1 µm are taken up via micropinocytosis [49]. Smaller particles (<100 nm) are internalized via clathrin-mediated or cavelae-mediated endocytosis. Further, positively charged nanogels are less cytocompatible than neutral or negatively charged particles [50]. Furthermore, the loaded biotherapeutics can be released from nanogels in a sustainable and controllable manner due to hydrolytic degradation of the network which in turn is dependent on the selected building blocks [51-52]. Importantly, triggered release of biotherapeutics from responsive nanogels can be acquired in response to biological stimuli (e.g. pH, enzymes and reducing agents) [42, 53-57]. Zhong et al. showed that 95% of cytochrome C loaded in reduction sensitive nanogels was released under reductive conditions. These nanogels loaded with this protein showed more cytotoxic effects against tumor cells compared to free cytochrome C [58]. Tang et al. developed enzyme responsive nanogels in which a polymeric shell composed of peptide crosslinker was formed by free radical polymerization on the surface of the protein. The entrapped protein can be released upon recognition and cleavage of the peptide crosslinker by furin, a peptidase present

in the Golgi apparat [59]. These features make nanogels attractive systems for anti-gen/vaccine delivery. In a recent study, Li *et al.* showed strong *in vivo* antitumor responses elicited by ovalbumin protein-loaded in nanogels. The strong features in that study were that the ovalbumin as a model antigen was very conveniently loaded into the pre-fabricated nanogels by electrostatic interactions, that the ovalbumin could subsequently be fixed into the nanogel by formation of a covalent disulfide bond between the protein and the nanogel network, and the protein was released by disulfide reduction in the lysosomes after internalization of the nanogels by dendritic cells. It was shown that these ovalbumin loaded cationic nanogels provoked robust antigen specific T-cell responses resulting in high percentage (40%) of regression of established tumor and substantial delay in tumor progression *in vivo* [60]. Therefore, these cationic nanogels are a potentially interesting delivery system for SLPs for cancer immunotherapy. Moreover, these nanogels have attractive advantages compared to other particulate systems in terms of loading of sensitive peptides during the manufacturing process. The peptides are loaded into the nanogels after particle formations (post-loading) which avoids possible unwanted modifications and aggregation of the peptides under harsh process conditions, e.g. the use of organic solvents and high shear forces, applied for the preparation of polymeric nanoparticles based on aliphatic polyesters of the PLGA/PLLA family of polymers.

In the present study, we explored the potency of SLP-loaded nanogels for the induction of T-cell responses. For that purpose, four SLPs covering CD8^{+} and CD4^{+} epitopes were synthesized and loaded both physically and chemically in cationic dextran-based nanogels. The formulated nanogels were characterized for size, zeta-potential and release profile *in vitro*. The capability of SLP loaded nanogels in priming antigen-specific T-cells was assessed *in vitro*. Finally, an *in vivo* study in mice was conducted to evaluate the antitumor immune response of these antigen-loaded nanogels.

RESULTS AND DISCUSSION

Peptide synthesis and characterization

Four peptides (CTL, Help, Cys-CTL and Cys-Help) were synthesized by solid-phase peptide synthesis (**Table 1**). The synthesized peptides were purified by Prep-HPLC to at least 90% purity and the obtained yields for the different peptides were approx. 40%. The UPLC chromatograms of the synthesized and purified peptides are shown in **Figure 1**. Mass spectroscopic analysis (**Figure 2**) showed that the main peaks eluting at approximately 5 min (**Figure 1A**), 9 min (Figure

1B), 13 min (**Figure 1C**) and 10 min (**Figure 1D**) correspond to CTL SLP, Cys-CTL SLP, Help SLP and Cys-Help SLP, respectively. To explain, MS analysis showed the $[M+2H]^{2+}$ of the main peaks at m/z 1317.7, 1369.3, 1232.1 and 1283.6 which are attributed to the masses of CTL SLP, Cys-CTL SLP, Help SLP and Cys-Help, respectively. In the MS experiment, DTT was added to the samples before analysis. Therefore no peaks attributed to the dimeric structures were observed, whereas when the samples were not treated with DDT, extra peaks were present in the chromatograms of Cys-CTL and Cys-Help (**Figure 1**) that according to MS correspond with the dimeric peptides formed due to the disulfide formation between the cysteine moieties. As listed in Table 1, the molecular masses of the different synthesized peptides measured by MS are similar to the theoretical values demonstrating that the aimed peptides were indeed obtained.
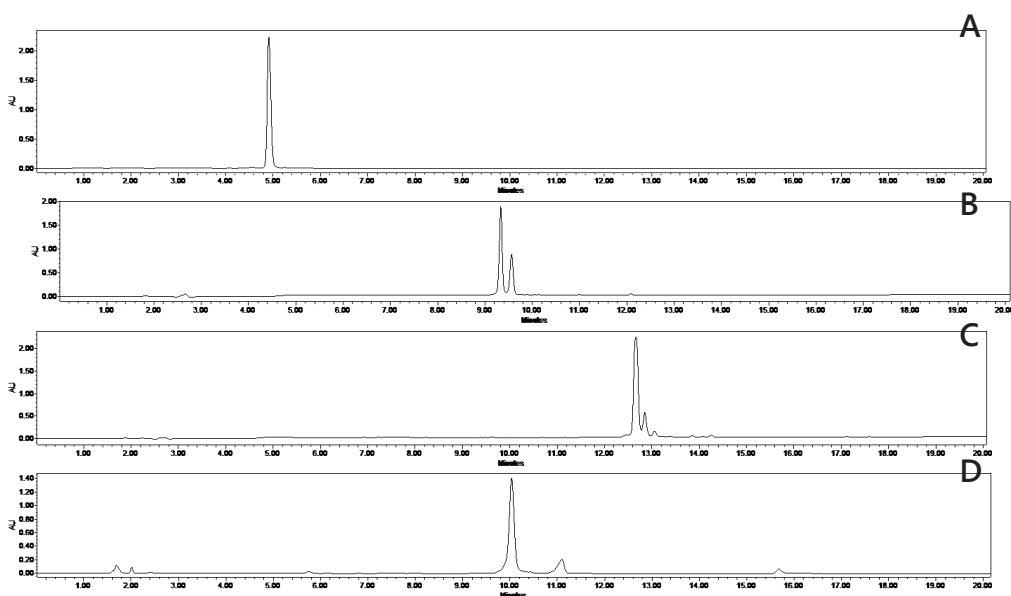
Figure 1. UPLC chromatograms of SLPs. A) Help, B) Cys-Help, C) CTL, D) Cys-CTL

Preparation and characterization of nanogel formulations

It has been shown that small nanoparticles (~200 nm) can be internalized by antigen presenting cells (APCs) and have a better ability to promote CD8+ T-cell immunity, which is crucial for immunotherapy of cancer [49-50]. Moreover, positively charged nanoparticles show the highest uptake by DCs. Therefore, in the present study, we were aiming to have a high loading and preferable particles that after loading still have a positive zeta-potential to allow uptake by DCs [71].
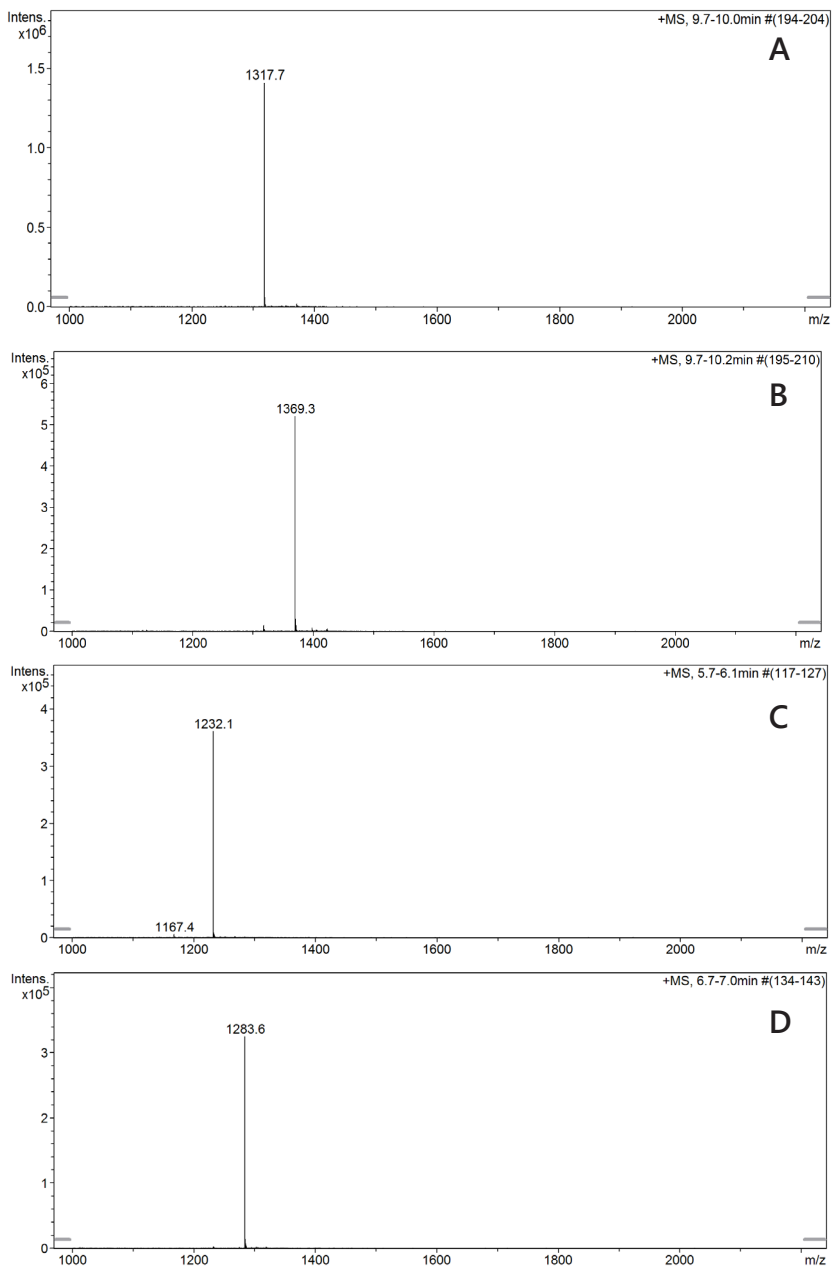
Figure 2. MS spectra of SLPs obtained via Fmoc solid phase peptide synthesis. A) CTL, B) Help, C) Cys-CTL, D) Cys-Help

Table 1. Characteristics of the synthesized peptides used in this study.

Peptide name	Peptide Sequence	Calculated molecular mass (g/mol)	Observed $[M+2H]^{2+}$ (g/mol)	Molecular mass (g/mol)*	Isoelectric point (PI)***
CTL	NH$_2$-DEWSGLEQLESIIN-FEKLAAAAAK-COOH	2633.9	1317.7	2633.4	3.9
** Cys-CTL	NH$_2$-CDEWSGLEQLESI-INFEKLAAAAAK-COOH	2737.1	1369.3	2736.6	3.9
Help	NH$_2$-DEWEISQAVHAA-HAEINEAGRE-COOH	2462.6	1232.1	2462.2	4.1
**Cys-Help	NH$_2$-CDEWEISQAVHAA-HAEINEAGRE-COOH	2565.7	1283.6	2565.2	4.1

*Determined by mass spectroscopy (ESI)

** Cysteine residue is located at the N-terminus of the peptide

*** Determined theoretically using an Innovagen peptide calculator program[70]

Following the inverse mini-emulsion technique [44, 57,] cationic dextran nanogels were obtained by exposing an emulsion of a dispersed water phase containing soluble polymer (dextran methacrylate) and monomers (TMAEMA, linker) in a continuous oil phase to UV irradiation, which resulted in photopolymerization of the methacrylate units. The average size of obtained empty nanogels was 207 nm and the nanogels showed positive zeta potential (+24.7 mV) which can be explained by copolymerization of TMAEMA monomers in the dextran network. After washing and freeze-drying, the photo-crosslinked nanogels were loaded both physically and covalently with the SLPs (CTL and Help) and Cys-SLPs (CTL and Help), respectively. The negatively charged peptides (pI values ~4, table 1) were absorbed into the cationic particles via electrostatic interactions, while the peptides containing a cysteine amino acid residue were additionally linked to the methacrylamide-disulfide linker that was present in the nanogels (Scheme 1). As shown in Table 2, the nanogels were physically loaded with a high efficiency with both peptides (CTL and Help) in a buffer of HEPES with low ionic strength (20 mm, pH 7.4). This demonstrates the capability of cationic nanogels for absorbing oppositely charged peptides exploiting electrostatic interactions as a driving force for the loading process. The obtained peptide-loaded nanogels were positively charged (zeta potential: +21-24 mV) and had an average size of about 210 nm and narrow size distribution (PDI <0.03).

The zeta potential of the nanogels slightly dropped from +24.7 to +22.6 mV and +24.6 mV for covalent CTL and Help, respectively, which is in agreement with a previous study where OVA was loaded into cationic nanogels[57]. This also

excludes that the peptides are adsorbed on the surface of the particles since then a negative zeta potential will be measured. Thus, the loading of the peptides had not affected the characteristics (size, charge) of the nanogels.

Table 3 shows that the CTL SLP was released from the nanogels in buffer of pH 7.4 containing 150 mM NaCl, indicating that under these high ionic strength conditions the electrostatic interactions between the polymer matrix and the absorbed peptides were broken. In contrast to CTL SLP, the Help SLP was not released in buffer of neutral pH and 150 mM NaCl. However, in a buffer of lower pH (150 mM NaCL, pH 4) the loaded peptide was quantitatively released in 2 hours demonstrating the pH-dependent release property of this peptide (Table 3). Importantly, nanogels loaded with both Cys-CTL and Cys-Help showed high loading even after two washings using the high ionic strength buffer (150 mM, pH 7 and 150 mM, pH 4 for CTL and Help, respectively, Table 2) demonstrating that these peptides were indeed immobilized/covalently linked to the nanogel network by thiol-disulfide exchange reaction as observed previously for thiolated ovalbumin and thiolated RNase [42, 57].
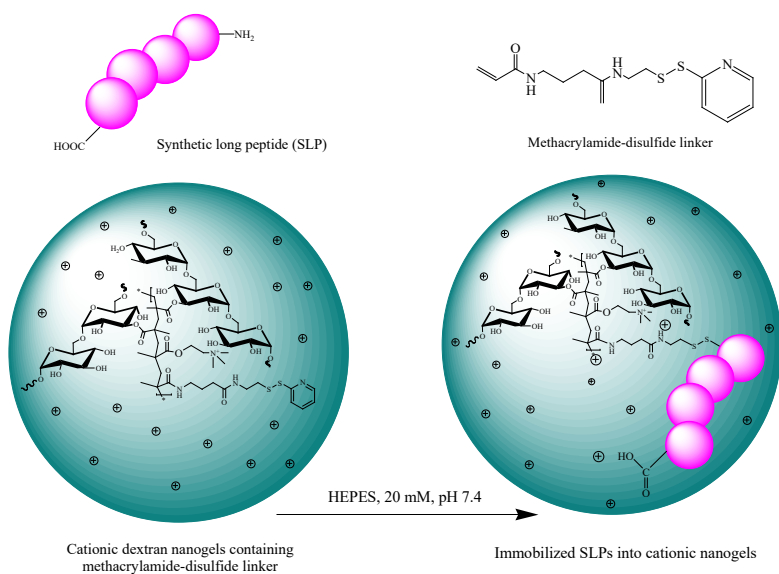
Scheme 1. Schematic representation of the cationic dextran nanogels containing *N*-(4-(2-(pyridine-2-yldisulfanyl)ethyl)-amidobutyl) methacrylamide as linker (left), and SLP loaded nanogels (right).

Table 2. Characteristics of SLP-loaded dex-MA-*co*-TMAEMA nanogels. Mean values with corresponding standard deviations of three independently prepared batches are shown.

Dex-MA-co-TMAEMA nanogels	Z_{ave} (nm)	ζ-potential (mV)	Loading efficiency [a] (%)	Loading content [b] (%)
Empty nanogels	207±3	+24.7±0.8	NA	NA
Non-covalent CTL-loaded nanogels	210±6	+23.0±0.9	100	15.0±0.0
Non-covalent Help-loaded nanogels	212±3	+24.3±1.0	100	15.0±0.0
Covalent CTL-loaded nanogels [c]	206±5	+22.6±0.3	86.7±0.5	13.7±0.1
Covalent Help-loaded nanogels [d]	215±2	+24.6±0.7	95.8±0.5	14.5±0.1

[a] Loaded peptide in nanogels/feed peptide weight x 100%

[b] Loaded peptide/dry peptide-loaded nanogels weight x 100%

[c] After washing with high ionic strength buffer of pH 7.4

[d] After washing with high ionic strength buffer of pH 4.0

Table 3. Percentage of released non-covalently bound peptides from nanogels in low and high ionic strength buffer of different pH. Mean values with corresponding standard deviations of three independently prepared batches are shown.

Samples	Released in HEPES 20 mM pH 7.4 (%)	Released in PBS 150 mM pH 7.4 (%)	Released in PBS 150 mM pH 4.0 (%)
Non-covalent CTL-loaded nanogels	0.0	98.7±7.7	NA
Non-covalent Help-loaded nanogels	0.0	0.0	95.5±3.9

To prove the triggered release of covalently linked peptides from cationic nanogels in reducing condition, CTL peptide and HELP peptide formulations were incubated in buffer containing glutathione as reducing agent. Figure 3 shows that upon addition of glutathione, triggered-release of peptides was observed (80% for Help SLP loaded nanogels and 100% for CTL SLP loaded nanogels) within 1 hour, revealing that the formed disulfide bonds between the linker present in the nanogels and cysteine groups of the N-terminus of the peptide were cleaved un-
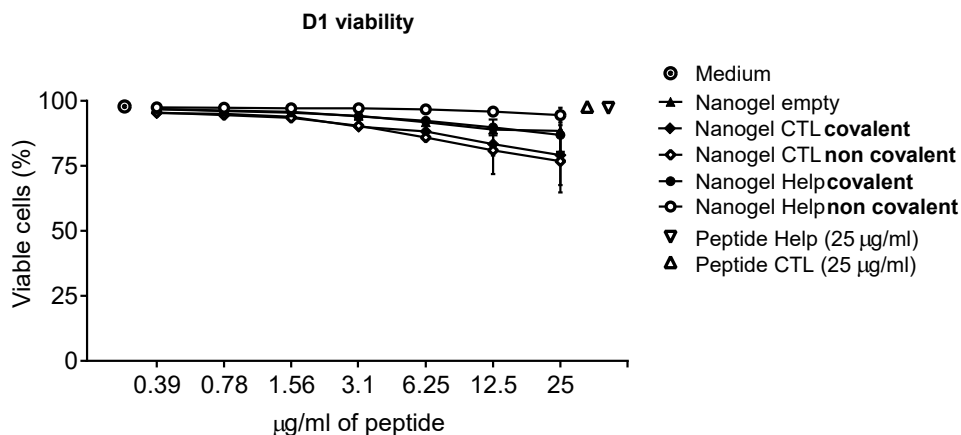
der these reducing conditions which lead to release of peptides from the nano-gels. This rapid triggered release from reduction-sensitive dextran nanogels is in line with our previous studies where proteins (ovalbumin or RNase A) were reversibly immobilized into cationic and anionic nanogels, respectively, via the same reducible linker [42, 57]. This release pattern results attractive for vaccination as the loaded peptides can be kept protected extracellularly and only released upon internalization due to the exposure to the endosomal reductive environ-ment.
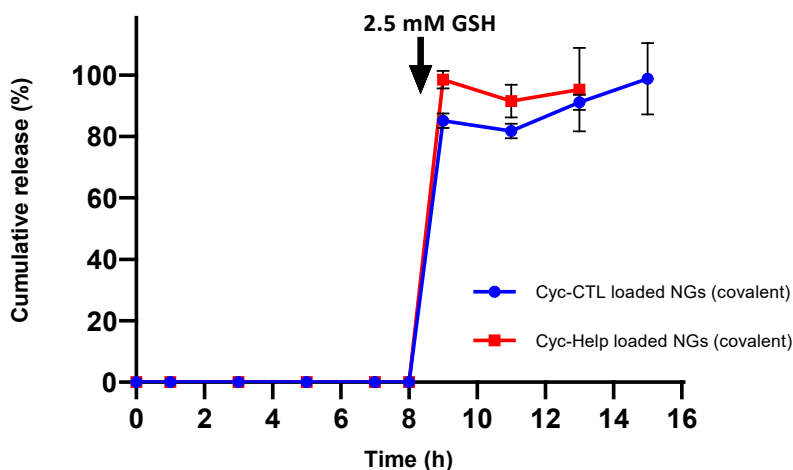
Figure 3. Release of Cys-Help and Cys-CTL from dex-MA-co-TMAEMA nanogels in PBS pH 4.0 and pH 7.4 at 37 C respectively; glutathione was added (2.5 mM final concentration) at 8 h. Data are shown as mean ± SD (n = 3).

Cytotoxicity and DC maturation

To determine the cytotoxicity of the different nanogel formulations, D1 dendritic cells were stimulated for 24 h at different concentrations of the free peptides as well as formulated in nanogels and cell viability and dendritic cell maturation were evaluated. Figure 4 shows that both peptides in their free form at the high-est concentration tested (25 g/mL) exhibited excellent cytocompatibility for D1 cells (viability > 95%). The nanogels (concentrations ranging from 2.7 to 175 g/mL were well-tolerated by DCs, which is in agreement with our previous stud-ies 50. However, at increasing concentrations (25 g/mL of peptide, 175 g/mL of nanogels) some toxicity was observed for covalent HELP peptide loaded nano-gels (viability 80%) and both CTL peptide formulations (viability 80%).

D1 viability

Viable cells (%) vs µg/ml of peptide

Legend:
- Medium
- Nanogel empty
- Nanogel CTL **covalent**
- Nanogel CTL **non covalent**
- Nanogel Help **covalent**
- Nanogel Help **non covalent**
- Peptide Help (25 µg/ml)
- Peptide CTL (25 µg/ml)

Figure 4. The viability of D1 cells, incubated for 24 h with free peptides (CTL and Help), non-covalent and covalent CTL peptide-loaded nanogels, non-covalent and covalent Help peptide-loaded nanogels. The colorimetric reading at 490 nm of nontreated cells were set at 100%; the data are shown as mean ± SD (n = 3).

Dendritic cells are susceptible to exogenous stimuli and can undergo maturation upon the encounter of foreign substances. This process leads to the upregulation of costimulatory molecules that in turn will enhance T cell activation. The ability of the nanogels to induce DC maturation was assessed by measuring the expression of the two costimulatory molecules, CD40+ and CD86+ (Figure 5)[72]. As expected, incubation of immature cells with LPS, as a positive control, resulted in increased CD40+ and CD86+ expression. There were no marked effects on DCs maturation in the presence of the free peptides (CTL and Help) while all nanogel formulations caused the up-regulation of co-stimulatory molecules (CD40+ and CD86+) in a concentration dependent manner. These data are in line with previous studies in which it was reported that positively charged particles are able to induce the maturation of DCs [73]. Maturation of DCs has a vital role in efficient DC-T cell interaction and of antigen-specific immune response initiation [20, 74].

In vitro antigen presentation

An essential step in the induction of a T cell response is the presentation of the epitopes on MHC I or MHC II molecules. The ability of dendritic cells to process and present the peptide upon nanogel-mediated uptake was investigated *in vitro* with the B3Z and OTIIZ T cell hybridoma reporter cell lines, which are specific respectively for the CTL and helper epitopes of OVA. Immature dendritic cells were pulsed for two hours with the free peptide or the different nanogels formulations and subsequently incubated with B3Z or OT IIZ cells for 24h.
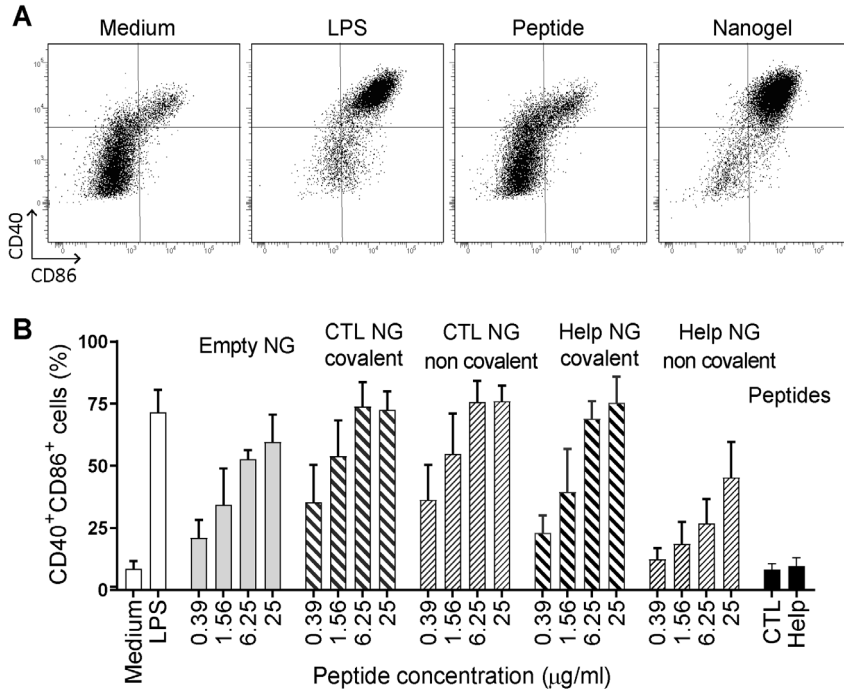
Figure 5. Nanogels induce maturation in DCs and upregulation of CD86+ and CD40+ co-stimulatory molecules. A. Representative dot plots for the expression of the costimulatory molecules CD40+ and CD86+ displayed for the highest concentration tested (25 µg/mL) after overnight incubation of D1 DCs . LPS (1 µg/mL) is used as positive control for DC maturation. **B.** Percentages of cells that upregulated CD40+ and CD86 after overnight incubation with titrated amounts of the indicated formulations. LPS (1 µg/mL) was used as positive control and soluble CTL and Help peptides (25 µg/mL) were used as controls. The data are shown as mean ± SD (n=3).

Antigen-dependent T cell activation was measured via a colorimetric assay. As shown in Figure 6A, the soluble peptides (CTL and Cys-CTL) display limited T cell activation, attributable to the poor cellular uptake of soluble peptide by DCs. In contrast, incubation of DCs with covalently conjugated CTL-loaded nanogels led to significantly enhanced activation of CD8+ T cells in a concentration-dependent manner. Moreover, this effect was dependent on the covalent attachment of the peptide to the nanogels, as the non-covalent CTL-loaded nanogels and physical mixtures of nanogels and soluble peptides did not result in an increase of T cell activation compared to free peptide. This could indicate that the non-covalent nanogels were not able to retain the peptide efficiently before uptake by the cells, whereas the nanogels with covalently immobilized peptide promote en-hanced uptake of the peptide which is released only under the reducing condi-

tions of the endosomes. These data are also in line with previous publications on OVA-conjugated nanogels in which it was shown that OVA can be delivered into DCs via the nanogel carrier and subsequently released intracellularly leading to antigen presentation and activation of CD8^{+} T cells [57, 60].

MHC class II presentation was also analyzed by detecting activation of OTIIZ. As shown in Figure 6B, all nanogel formulations display enhanced MHC II antigen presentation compared to free soluble peptide, differently from what observed with class I presentation. This effect is at least partially independent from the disulfide bond as both the non-covalently loaded nanogels as well as the mixture of helper peptide and empty nanogels already display increased OTIIZ activation. This could be explained by an overall increased uptake of the peptide that is still retained in the nanogels. However, the covalently loaded nanogels still yield the highest activation, indicating that peptide protection by nanogels before uptake is indeed occurring and that intracellular release allows efficient MHC II presentation.
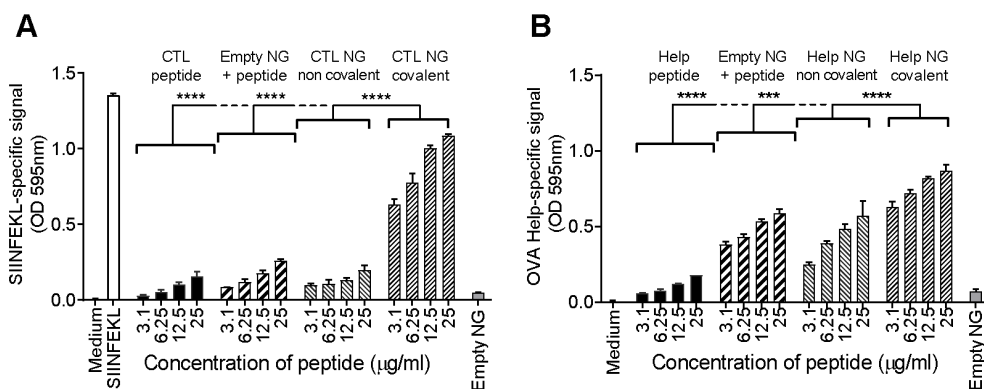
Figure 6. **Enhanced MHC class I and class II presentation upon nanogel-mediated uptake of peptide A.** MHC class I presentation of nanogel-formulated CTL peptide by DCs was analyzed by measuring the activation of B3Z hybridoma CD8^{+} T cell line upon overnight incubation with DCs pulsed for 2 hours with titrated amounts of the indicated formulations. SIINFEKL peptide (100 ng/mL) was used as positive control. **B.** MHC class II presentation of nanogel-formulated Help peptide was analyzed by measuring the activation of the OTIIZ hybridoma CD4^{+} T cell line upon overnight incubation with DCs pulsed for 2 hours with titrated amounts of the indicated formulations. For both A and B, each bar represents the average of triplicates with SD. Statistical significance of the differences between the different formulations at every concentration was determined by 2-way ANOVA followed by multiple comparison and Dunnet correction. The experiment was repeated three times with similar outcomes.

In conclusion, *in vitro* evaluation of nanogels as peptide carriers on DCs exhibit low toxicity and maturating properties. Moreover, the covalent attachment of the peptide to the nanogel via a disulfide link results functional for peptide retention into the nanogels until arrival to the endosomes, where peptide can be released to enter both the class I and class II presentation pathways.

In vivo induction of CD8+ T cells

We observed that covalently loaded nanogels promote uptake of peptide by DCs and increased antigen presentation, the potency of peptide-loaded nanogels to induce *de novo* T cell-mediated immunity was investigated *in vivo*. Mice were injected intradermally with different nanogel formulations containing SLPs and poly(I:C) as adjuvant[20]. As nanogels were able to induce *in vitro* DC maturation, the potential of covalently loaded nanogels as a self-adjuvating vaccine was also investigated. Mice received a prime and booster immunization on day 0 and 14 respectively. The SIINFEKL-specific CD8+ T cell responses could be monitored in blood via SIINFEKL/H2-Kb tetramer staining. As presented in Figure 7A, at day 9 after the prime immunization, vaccination with only the CTL SLPs raises little CD8+ responses. However, covalent loading of the same peptide into nanogels significantly enhance T cell induction. The addition of a helper epitope and therefore a CD4+ T cell helper response greatly enhances the induction of specific CD8+ T cells, as observed in mice vaccinated with combination of CTL and Help peptide. The combination of adjuvanted covalent CTL and Helper nanogels induces the highest responses for SIINFEKL. Furthermore, the addition of an adjuvant is important for optimal induction, as the nonadjuvanted group displays no induction. Importantly, the nanogels with covalently immobilized peptides adjuvanted with poly (I:C) showed superior CD8+ T cell responses activation as compared to nanogels physically loaded with the peptides (both adjuvanted with poly (I:C)), again indicating the key role of covalent conjugation of peptides to the nanogels.

One week after the booster injection (on day 22), the CD8+ T cell responses in blood samples were analyzed again quantitatively. Booster injection induced an overall increase of the magnitude of SIINFEKL-specific CD8+ responses in all groups, except the one vaccinated with CTL peptide only, underlining the importance of CD4+ T cell help for optimal CD8+ induction. Notably, nanogel-formulated CTL peptide display responses comparable to the peptide group that contains both the CTL and the Helper epitopes, highlighting the importance of the method of peptide delivery for optima T cell induction. This is especially evident in the
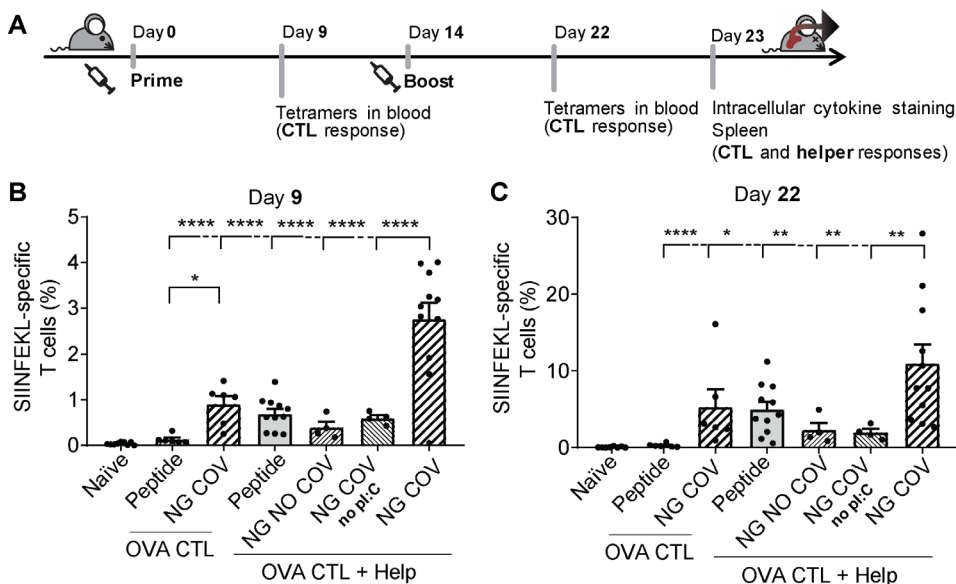
combination group of CTL and Help covalent loaded nanogels. Non covalently loaded nanogel do not achieve the same effect and it can be concluded that, although the peptide-loaded nanogels showed effective DC maturing properties *in vitro* (Figure 5), a strong TLR ligand adjuvant (poly(I:C)) was needed to achieve a strong DC activation *in vivo*.


Figure 7. Peptide vaccination with covalently loaded nanogels enhances induction of CTL responses A. Schematic overview of the vaccination experiment. All groups were vaccinated intradermally twice at interval of two weeks with 10 µg of the indicated peptide (CTL or Help) or a mixture of both and adjuvanted with 20 µg of poly(I:C), except for the nonadjuvanted group (NG COV no poly(I:C)). The induction of CTL responses was monitored in blood by SIINFEKL-Kb tetramer staining at day 9 and day 22. At day 23 spleens were harvested to analyze both CTL and helper responses via intracellular cytokine staining. **B** and **C.** Levels of SIINFEKL-specific CD8+ T cells as percentages of total CD8+ T cells upon tetramer staining in blood after prime (day 9, panel B) and booster (day 22, panel C) vaccine injections. Statistical significance was determined by one-way ANOVA followed by multiple comparison and Bonferroni correction. *: $p < 0.05$, **: $p < 0.01$, ***: $p < 0.001$, ****: $p < 0.0001$

Upon antigen recognition, CTL T cells produce different cytokines that are important for their functions, the most important being IFNγ and TNFα. Therefore, mice were sacrificed at day 23, and OVA-specific CD8+ and CD4+ T cells responses were both analyzed in cells harvested from spleens upon intracellular cytokine staining (ICS).The number of CD8+ T cells in the spleen producing these two cytokines in response to SIINFEKL displays a similar response among groups

as observed in blood via tetramer staining (Figure 8A). Double TNFα and IFNγ producers are indicators of the quality of the response, as the ability of producing both cytokines is associated with improved differentiation and effector functions. Notably, we observe that the highest percentage of double producers is observed in the adjuvanted covalent-loaded nanogels group when CTL and helper peptides are combined (Figure 8B).

Cytokine staining also allows quantification of CD4+ T cell helper responses, by staining of IFNγ and IL-2 producing cells. All groups exhibit similar amount of OVA-specific CD4+ T cell responses (Figure 8C), and the nanogel seem to only partially increase the overall amount of Help responses. However, when looking at the quality of T cells in terms of single or double producer, the covalently loaded nanogel exhibit the most efficient T cell responses with the highest percentage of total double producers (Figure 8D).
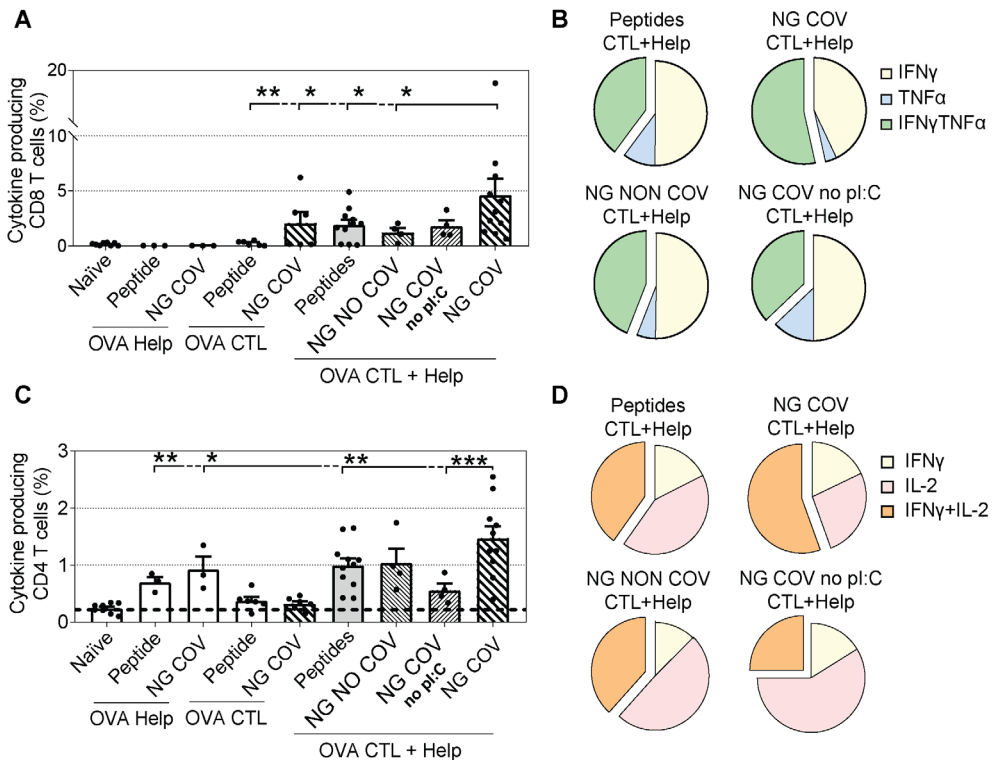
Figure 8. Vaccination with nanogel-formulated peptides induces higher quality CD8+ and CD4+ T cell responses. A-D Splenocytes from vaccinated mice were incubated ex vivo with CTL and Help peptide-loaded DCs and cytokine producing CD8+ (**A**) and CD4+ (**C**) were detected via intracellular cytokine staining. The average percentage of single or double cytokine producers among cytokine producing CD8+ (**B**) and CD4+ (**D**) T cells is represented.

CONCLUSIONS

In this study, we demonstrated the potential of cationic dextran nanogels to induce antigen-specific immune responses. SLP conjugated nanogels were internalized by DCs and activated these immature cells and subsequently boost the antigen presentation *in vitro*. An *In vivo* study showed that the covalently conjugated peptide nanogels in the presence of poly I:C can effectively stimulate strong functional CD8^{+} and CD4^{+} responses in comparison to naked SLP and non-conjugated formulations, indicating the key role of reducible covalent bond for intracellular delivery of vaccine peptides. Therefore, cationic dextran nanogels are promising carriers as vaccine formulations for cancer immune therapy.

MATERIAL AND METHODS

Materials. Dextran (from Leuconostoc ssp) Mw=40,000 Da, glycidyl methacrylate (GMA) and hydroxyethyl methacrylate (HEMA) were obtained from Sigma Chemical Co. (St. Louis, MO, USA). Methacrylate-derivatized dextran (dex-MA) with a degree of substitution of 8 (DS, i.e. a number of MA groups per 100 glucopyranose units as analyzed by ^{1}H-nuclear magnetic resonance (NMR) spectroscopy) was synthesized as described by van Dijk-Wolthuis *et al.* [61-62]. [2-(Methacryloyloxy)-ethyl] trimethylammonium chloride (TMAEMA, 80 wt % solution in water) and light mineral oil (M8410) were purchased from Sigma (St. Louis, MO, USA). ABIL EM 90 and Irgacure 2959 were purchased from Goldschmidt (Essen, Germany) and Ciba Specialty Chemicals (Hercules, USA), respectively. Fmoc-amino acids were obtained from Iris Biotech GmbH (Germany). Acetone, acetonitrile, dimethyl sulfoxide, n-hexane and trifluoroacetic acid (TFA), HBTU/HOBt and *N,N*-diisopropylethylamine were products of Biosolve (Valkenswaard, the Netherlands). Glutathione, thioanisole, 1,4-Dithiothreitol (DTT), ethanedithiol (EDT) and anisole were obtained from Sigma-Aldrich (Zwijndrecht, the Netherlands). *N*-2-hydroxyethylpiperazine-*N*'-2-ethanesulfonic acid (HEPES) was purchased from Acros Chimica (Geel, Belgium). Phosphate buffer saline (Na+ 163.9 mM, Cl- 140.3 mM, HPO42- 8.7 mM, H2PO4- 1.8 mM, pH 7.4) was purchased from Braun (Germany). Chlorophenol red-β-D-galactopyranoside was acquired from Sigma (St. Louis, MO, USA). Chlorophenol red-β-d-galactopyranoside (CPRG) was provided by Merck (Darmstadt, Germany). All other chemicals used were obtained from commercial suppliers and were of analytical grade. *N*-(4-(2-(pyridine-2-yldisulfanyl)ethyl)-amidobutyl) methacrylamide was synthesized as described previously [57].

Cell lines. D1 cells, a long-term growth factor-dependent immature myeloid dendritic cell line of splenic origin derived from a female C57BL/6 mouse was cultured at 37°C with 5% CO_2 in IMDM (Iscove's Modified Dulbecco's Medium, Lonza) [63]. B3Z, a $CD8^+$ T cell hybridoma specific for the SIINFEKL epitope of OVA [64] was maintained in IMDM (Iscove's Modified Dulbecco's Medium, Lonza) supplemented with 100 IU/mL penicillin/streptomycin (Gibco™, Bleiswijk, the Netherlands), 2 mM glutamine (Gibco, Bleiswijk, the Netherlands), 25 μM 2-mercaptoethanol and 500 μg/mL Hygromycin B (AG Scientific, San Diego, USA).

Mice. Female C57BL/6 (H-2b) mice were obtained from Charles River Laboratories (L'Arbresle, France) and kept under standardized conditions in the Leiden University Medical Centre animal facility. The *in vivo* experiment as described in section 2.8 was carried out according to the Dutch Experiments on Animal Act, which serves the implementation of "Guidelines on the protection of experimental animals" by the Council of Europe.

Synthesis of SLPs. The peptide epitopes (Table 1) were synthesized by standard Fmoc solid phase peptide synthesis using a Symphony peptide synthesizer (Symphony; Protein Technologies, Tucson, AZ, United States) using protocols as described by Coin *et al.* [65]. In brief, *N*-methyl-2-pyrrolidone (NMP) was used as a coupling and washing solvent during the synthesis process. For each coupling step, Fmoc-amino acids were activated by 4 eq HBTU/HOBt and 8 eq *N,N*-diisopropylethylamine to react with the free N-terminal amino acids present on the resin (Sigma-Aldrich, the Netherlands) for one hour. After each coupling step, the Fmoc groups were removed by four times treatment of 20% piperidine in NMP for ten minutes. Reagent R TFA/thioanisole/EDT/anisole (90/5/3/2) was used to simultaneously cleave the peptide off from the resin and remove the side chain protecting groups. The synthesized peptides were purified by Prep-HPLC using Reprosil-Pur C18 column (10 μm, 250 × 22 mm) eluted with water-acetonitrile gradient from 5 to 80% acetonitrile (10 mM ammonium bicarbonate, pH 8.3) in 40 minutes at a flow-rate of 15 mL/min with UV detection at 220 nm. Fractions of 30 mL were collected, and the purity was confirmed by analytical UPLC using Waters XBridge C18 column eluted with water-acetonitrile gradient 5 to 80% ACN (10 mM ammonium bicarbonate, pH 8.3) in 8 minutes at flow rate 1 m/min and UV detection at 280 and 220 nm.

LC–MS analysis was carried out using an Acquity UPLC system, (Waters Corporation, Milford, USA) combined with an Agilent Technologies 6300 Series LC/MSD ion-trap mass spectrometer (Santa Clara, CA, USA) in the positive ion mode.

A gradient was used with a mobile phase A (95% H_2O, 5% ACN plus 0.1% formic acid) and a mobile phase B (100% ACN plus 0.1% formic acid). Elution was done at room temperature using a BEH300 C18 1.7 µm column. The eluent linearly changed from 100% A to 100% B in 20 min with a flow rate of 1 mL/min. The MS settings were: capillary voltage, 2 kV; nebulizer pressure, 60 psi; dry gas flow, 11 L/min; dry gas temperature, 350 ℃; scan range, m/z 50–2000. To prevent disulfide bond formation between the two cysteine residues in peptides (Cys-CTL and Cys-Help), dithiothreitol (10 mg/mL) was added to the peptides before MS analysis.

Preparation and characterization of peptide-loaded nanogels. Cationic nanogels were prepared by inverse mini-emulsion technique as previously described [44, 57]. In brief, an emulsion with aqueous droplets containing 120 mg of methacrylated dextran (DS 8), trimethyl aminoethyl methacrylate (160 µL) and the pyridyldisulfide-containing methacrylamide monomer, *N*-(4-(2-(pyridine-2-yldisulfanyl)ethyl)-amidobutyl)methacrylamide synthesized as described previously [57], (27 mg) was photo-polymerized (Bluepoint UV source, 60% amplitude, 940 mW/cm^2 , Hönle UV technology, Germany) for 15 min. Particles were washed with acetone and four times with acetone/hexane (1:1, v/v) to remove the used mineral oil and surfactant. Finally, nanoparticles were collected by redispersion in water and freeze drying. To covalently conjugate Cys-peptides to the nanogel network (covalent NGs), 4.25 mL of a suspension of cationic nanogels (4 mg/mL) in HEPES buffer (20 mM, pH 7.4) was mixed with 750 l peptide solutions (4 mg/mL) and incubated overnight at room temperature. To remove non-reacted peptides, the particles were washed twice with high ionic strength buffer (PBS 150 mM,pH 7.4) and the final pellets obtained after centrifugation (15,000 rpm, 1h) were washed with water and subsequently lyophilized. The physically loaded nanogels (non-covalent NGs) were prepared by adding the peptides lacking cysteine residues (Table 1, CTL and Help) to the particle dispersions in a HEPES buffer solution (20 mM, pH 7.4). After overnight incubation at room temperature, the particles were recovered by centrifugation (15,000 rpm, 1h), subsequently washed with water and lyophilized. The particle size and zeta potential of the obtained particles were measured in HEPES (10 mM, pH 7.4) using DLS (Malvern ALV/CGS-3 Goniometer, Malvern Instruments, Malvern, UK) and Zetasizer (Zetasizer Nano, Malvern Instruments, USA), respectively.

In vitro release. To study the release of SLP from the nanogels, freeze-dried CTL SLP-loaded and Help SLP-loaded nanogels (5 mg/mL) were suspended in

PBS (Na$^+$ 163.9 mM, Cl$^-$ 140.3 mM, HPO$_4^{2-}$ 8.7 mM, H$_2$PO4$^-$ 1.8 mM) at pH 7.4 or pH 4.0, and incubated at 37 °C. At different time points, 3 samples were taken and centrifuged (15,000 rpm, 1 h) and the collected supernatants were subsequently analyzed by reversed-phase ultrahigh-performance liquid chromatography (RP_UPLC) for peptide quantification. To trigger release of the immobilized peptides, glutathione at a final concentration of 2.5 mM was added to the nanogel dispersion and the obtained supernatants after centrifugation (15,000 rpm, 1 h) were analyzed for concentration of peptides using UPLC (Acquity UPLC, Waters Corporation, Milford, USA) equipped with a BEH300 C18 1.7 μm column. Solvent mixtures consisting of 100% H$_2$O/0.05% TFA and 100% ACN/0.04% TFA were used as eluent A and B, respectively. A gradient was run from 5 to 70% B at a flow rate of 1 mL/min. The injection volume was 7.5 μl and the detection wavelength was 280 nm. The calibration curve was linear between 10 to 1000 μg/mL CTL and Help SLP peptides.

Cell viability and DC maturation. D1 cells (100,000 cells/well) were seeded in 96-well round-bottomed plates and incubated with empty nanogels, non-covalent NGs (loaded with CTL and Help peptides), covalent NGs (loaded with CTL and Help peptides) and soluble peptides (CTL and Help) at indicated concentrations (range 0.39-25 μg mL^{-1}) in culture medium. After 24 h of incubation, the relative cell viability and dendritic cell maturation were assessed by 7-aminoactinomycin D exclusion and staining with fluorescent antibodies directed against CD86$^+$ and CD40$^+$ (eBioscience, Landsmeer, the Netherlands) followed by acquisition by BD^{TM} LSR II flow cytometer.

In vitro antigen presentation. The immunogenicity of the peptide-loaded nanogels was evaluated by an *in vitro* T hybridoma assay [64]. In detail, immature D1 cells (50,000 cells/well) were incubated in 96-well flat-bottomed plates in supplemented IMDM with peptide-loaded nanogels (non-covalent and covalent) or soluble peptides (CTL and Help) in PBS (composition given in section 2.1) at 37 °C and at different concentrations (0.39-25 g/mL of peptide). After 2 h, the cells were washed with supplemented IMDM culture medium in order to remove excess antigen. Subsequently, 50,000/well B3Z T, a CD8$^+$ T cell hybridoma cell or OTIIZ, a CD4$^+$ T-cell hybridoma cell line both producing a β-galactosidase construct upon TCR triggering, were added followed by overnight incubation at 37 °C. MHC class I and II antigen presentation was measured indirectly by a colorimetric assay using chlorophenol red-β-d-galactopyranoside (CPRG) and the color conversion was detected by measuring absorbance at 595 nm [66-67].

Immunization of mice. Mice were immunized by intradermal injections of the formulations in the tail base area. All formulations were prepared at the day of injections and consisted of 10 µg of the different peptides (CTL, Help or both combined) in a total volume of 30 µl PBS (composition given in section 2.1). The nanogel vaccines were adjuvanted with 20 µg of poly(I:C) (InvivoGen, Toulouse, France). Immunization was performed at day 0 (prime injection) and at day 14 (booster injection). During the study, blood samples were collected from the tail vein at day 8 and 22 to monitor T cell responses. At day 23, spleens were harvested for *ex vivo* analysis of $CD8^+$ and $CD4^+$ T cell responses[68].

Analysis of antigen-specific CD8 and CD4 T cell responses. For detection of SIINFEKL-specific $CD8^+$ T cells, surface staining was performed on blood samples after red blood cell lysis. Cells were washed using staining buffer and incubated for 15 minutes at room temperature with labelled SIINFEKL-tetramers. After 15 minutes, cells were incubated on ice and a mix containing 7-aminoactinomycin D (Life Technologies, for viability staining) and fluorescently labelled antibodies against $CD8^+$ (BioLegend, San Diego, USA) and $CD3^+$ (eBioscience, Landsmeer, the Netherlands) was added[69]. Intracellular cytokine analysis of splenocytes was performed after incubating the cells for 5-6 hours with previously loaded nanogels (with 2 µg/mL of CTL and Help peptide), in presence of the protein transport inhibitor Brefeldin A (10 µg/mL, BD Biosciences, Breda, the Netherlands). After incubation, the cells were stained for surface markers $CD3^+$, $CD8^+$ and $CD4^+$ and fixed overnight in 0.1% paraformaldehyde. Next day, permeabilization and intracellular staining of IFNγ, TNFα and IL-2 was performed and the samples were subsequently analyzed on BD^{TM} LSR II flow cytometer as described previously[69].

Statistical analysis. Graph Pad Prism software version 7 was used for statistical analysis. Two-way analysis of variance (ANOVA) tests was used to evaluate the induced $CD8^+$ and $CD4^+$ T-cell responses and cytokine production *in vivo*. Statistical significance is considered when $p < 0.05$.

REFERENCES

[1] Shanker, A.; Marincola, F. M., Cooperativity of adaptive and innate immunity: implications for cancer therapy. Cancer Immunology, Immunotherapy : CII, 60 (8): 1061-74, 2011.

[2] Bos, R.; Sherman, L. A., CD4+ T-cell help in the tumor milieu is required for recruitment and cytolytic function of CD8+ T lymphocytes. Cancer Research, 70 (21): 8368-77, 2010.

[3] Koury, J.; Lucero, M.; Cato, C.; Chang, L.; Geiger, J.; Henry, D.; Hernandez, J.; Hung, F.; Kaur, P.; Teskey, G.; Tran, A., Immunotherapies: Exploiting the immune system for cancer treatment. J Immunol Res. (4):9585614, 2018.

[4] Palucka, K.; Ueno, H.; Fay, J.; Banchereau, J., Dendritic cells and immunity against cancer. Journal of Internal Medicine, 269 (1): 64-73, 2011.

[5] Palucka, K.; Banchereau, J., Dendritic-cell-based therapeutic cancer vaccines. Immunity, 39 (1): 38-48, 2013.

[6] Mantia-Smaldone, G. M.; Chu, C. S., A review of dendritic cell therapy for cancer: progress and challenges. BioDrugs, 27 (5): 453-68, 2013.

[7] Hu, Z.; Ott, P. A.; Wu, C. J., Towards personalized, tumour-specific, therapeutic vaccines for cancer. Nature Reviews Immunology, 18, 168-182, 2017.

[8] Banchereau, J.; Palucka, K., Cancer vaccines on the move. Nature Reviews Clinical Oncology,15, 9-10, 2017.

[9] Bijker, M. S.; Melief, C. J.; Offringa, R.; van der Burg, S. H., Design and development of synthetic peptide vaccines: past, present and future. Expert Review of Vaccines, 6 (4): 591-603, 2007.

[10] Melief, C. J.; van der Burg, S. H., Immunotherapy of established (pre)malignant disease by synthetic long peptide vaccines. Nature Reviews. Cancer, 8 (5): 351-360, 2008.

[11] Sabbatini, P.; Tsuji, T.; Ferran, L.; Ritter, E.; Sedrak, C.; Tuballes, K.; Jungbluth, A. A.; Ritter, G.; Aghajanian, C.; Bell-McGuinn, K.; Hensley, M. L.; Konner, J.; Tew, W.; Spriggs, D. R.; Hoffman, E. W.; Venhaus, R.; Pan, L.; Salazar, A. M.; Diefenbach, C. M.; Old, L. J.; Gnjatic, S., Phase I trial of overlapping long peptides from a tumor self-antigen and poly-ICLC shows rapid induction of integrated immune response in ovarian cancer patients. Clinical Cancer Research, 18 (23): 6497-508, 2012.

[12] Rosalia, R. A.; Quakkelaar, E. D.; Redeker, A.; Khan, S.; Camps, M.; Drijfhout, J. W.; Silva, A. L.; Jiskoot, W.; van Hall, T.; van Veelen, P. A.; Janssen, G.; Franken, K.; Cruz, L. J.; Tromp, A.; Oostendorp, J.; van der Burg, S. H.; Ossendorp, F.; Melief, C. J., Dendritic cells process synthetic long peptides better than whole protein, improving antigen presentation and T-cell activation. European Journal of Immunology, 43 (10): 2554-65, 2013.

[13] Black, M.; Trent, A.; Tirrell, M.; Olive, C., Advances in the design and delivery of peptide subunit vaccines with a focus on toll-like receptor agonists. Expert Review of Vaccines, 9 (2): 157-73, 2010.

[14] Skwarczynski, M.; Toth, I., Peptide-based synthetic vaccines. Chemical Science, 7 (2): 842-854, 2016.

[15] Li, W.; Joshi, M. D.; Singhania, S.; Ramsey, K. H.; Murthy, A. K., Peptide vaccine: progress and challenges. Vaccines, 2 (3): 515, 2014.

[16] Irvine, D. J.; Hanson, M. C.; Rakhra, K.; Tokatlian, T., Synthetic nanoparticles for vaccines and immunotherapy. Chemical Reviews, 115 (19): 11109-11146, 2015.

[17] De Geest, B. G.; Willart, M. A.; Hammad,

H.; Lambrecht, B. N.; Pollard, C.; Bogaert, P.; De Filette, M.; Saelens, X.; Vervaet, C.; Remon, J. P.; Grooten, J.; De Koker, S., Polymeric multilayer capsule-mediated vaccination induces protective immunity against cancer and viral infection. ACS Nano, 6 (3): 2136-49, 2012.

[18] Chen, W.; Huang, L., Induction of cytotoxic T-lymphocytes and antitumor activity by a liposomal lipopeptide vaccine. Molecular Pharmaceutics, 5 (3): 464-71, 2008.

[19] Dimier-Poisson, I.; Carpentier, R.; N'Guyen, T. T.; Dahmani, F.; Ducournau, C.; Betbeder, D., Porous nanoparticles as delivery system of complex antigens for an effective vaccine against acute and chronic Toxoplasma gondii infection. Biomaterials, 50: 164-175, 2015.

[20] Varypataki, E. M.; van der Maaden, K.; Bouwstra, J.; Ossendorp, F.; Jiskoot, W., Cationic liposomes loaded with a synthetic long peptide and poly(I:C): a defined adjuvanted vaccine for induction of antigen-specific T cell cytotoxicity. The AAPS Journal, 17 (1): 216-226, 2015.

[21] Rosalia, R. A.; Cruz, L. J.; van Duikeren, S.; Tromp, A. T.; Silva, A. L.; Jiskoot, W.; de Gruijl, T.; Lowik, C.; Oostendorp, J.; van der Burg, S. H.; Ossendorp, F., CD40-targeted dendritic cell delivery of PLGA-nanoparticle vaccines induce potent anti-tumor responses. Biomaterials, 40: 88-97, 2015.

[22] Sun, Q.; Barz, M.; De Geest, B. G.; Diken, M.; Hennink, W. E.; Kiessling, F.; Lammers, T.; Shi, Y., Nanomedicine and macroscale materials in immuno-oncology. Chemical Society Reviews, 48 (1): 351-381, 2019.

[23] Aucouturier, J.; Ascarateil, S.; Dupuis, L., The use of oil adjuvants in therapeutic vaccines. Vaccine, 24 Suppl 2, S2-44-5, 2006.

[24] Aucouturier, J.; Dupuis, L.; Deville, S.; Ascarateil, S.; Ganne, V., Montanide ISA 720 and 51: a new generation of water in oil emulsions as adjuvants for human vaccines. Expert review of vaccines, 1 (1): 111-118, 2002.

[25] Kenter, G. G.; Welters, M. J.; Valentijn, A. R.; Lowik, M. J.; Berends-van der Meer, D. M.; Vloon, A. P.; Drijfhout, J. W.; Wafelman, A. R.; Oostendorp, J.; Fleuren, G. J.; Offringa, R.; van der Burg, S. H.; Melief, C. J., Phase I immunotherapeutic trial with long peptides spanning the E6 and E7 sequences of high-risk human papillomavirus 16 in end-stage cervical cancer patients shows low toxicity and robust immunogenicity. Clinical Cancer Research, 14 (1): 169-77, 2008.

[26] Schwartzentruber, D.J.; Lawson, D.H.; Richards, J.M. ; Conry, R.M.; Miller, D.M.; Treisman, J.; Gailani, F.; Riley, L.; Conlon, K.; Pockaj, B.; Kendra, K.L.; White, R.L.; Gonzalez, R.; Kuzel, T.M.; Curti, B.; Leming, P.D.; Whitman, E.D.; Balkissoon, J.; Reintgen, D.S.; Kaufman, H.; Marincola, F.M.; Merino, M.J.; Rosenberg, S.A.; Choyke, P.; Vena, D.; Hwu, P., gp100 peptide vaccine and interleukin-2 in patients with advanced melanoma. The New England Journal of Medicine, 364 (22): 2119-2127, 2011.

[27] Oka, A. Tsuboi, T. Taguchi, T. Osaki, T. Kyo, H. Nakajima, O.A. Elisseeva, Y. Oji, M. Kawakami, K. Ikegame, N. Hosen, S. Yoshihara, F. Wu, F. Fujiki, M. Murakami, T. Masuda, S. Nishida, T. Shirakata, S. Nakatsuka, A. Sasaki, K. Udaka, H. Dohy, K. Aozasa, S. Noguchi, I. Kawase, H. Sugiyama, Induction of WT1 (Wilms' tumor gene)-specific cytotoxic T lymphocytes by WT1 peptide vaccine and the resultant cancer regression. Proceedings of the National Academy of Sciences of the United States of America, 101 (38): 13885-13890, 2004.

[28] Hailemichael, Y.; Dai, Z.; Jaffarzad, N.; Ye, Y.; Medina, M.A.; Huang, X.F.; Dorta-Estremera, S.M.; Greeley, N.R.; Nitti, G.; Peng, W.; Liu, C.; Lou, Y.; Wang, Z.; Ma, W.; Rabinovich, B.; Sowell, R.T; Schluns, K.S.; R.E. Davis, R.E.; Hwu, P.; Overwijk, W.W.; Persistent antigen at vaccination sites induces tumor-specific CD8(+) T cell sequestration, dysfunction and deletion. Nature Medicine, 19 (4): 465-472, 2013.

[29] Cruz, L. J.; Tacken, P. J.; Fokkink, R.; Joost-

en, B.; Stuart, M. C.; Albericio, F.; Torensma, R.; Figdor, C. G., Targeted PLGA nano- but not microparticles specifically deliver antigen to human dendritic cells via DC-SIGN in vitro. Journal of Controlled Release, 144 (2): 118-26, 2010.

[30] Fischer, S.; Schlosser, E.; Mueller, M.; Csaba, N.; Merkle, H. P.; Groettrup, M.; Gander, B., Concomitant delivery of a CTL-restricted peptide antigen and CpG ODN by PLGA microparticles induces cellular immune response. Journal of Drug Targeting, 17 (8): 652-61, 2009.

[31] Rahimian, S.; Fransen, M. F.; Kleinovink, J. W.; Amidi, M.; Ossendorp, F.; Hennink, W. E., Particulate systems based on poly(lactic-co-glycolic)acid (pLGA) for immunotherapy of cancer. Current Pharmaceutical Design, 21 (29): 4201-4216, 2015.

[32] Rad-Malekshahi, M.; Fransen, M. F.; Krawczyk, M.; Mansourian, M.; Bourajjaj, M.; Chen, J.; Ossendorp, F.; Hennink, W. E.; Mastrobattista, E.; Amidi, M., Self-assembling peptide epitopes as novel platform for anticancer vaccination. Molecular Pharmaceutics, 14 (5): 1482-1493, 2017.

[33] Black, M.; Trent, A.; Kostenko, Y.; Lee, J.S.; Olive, C.; Tirrell, M.; Self-assembled peptide amphiphile micelles containing a cytotoxic T-cell epitope promote a protective immune response in vivo. Advanced Materials, 24(28):3845-3849, 2012.

[34] Silva, A. L.; Rosalia, R. A.; Sazak, A.; Carstens, M. G.; Ossendorp, F.; Oostendorp, J.; Jiskoot, W., Optimization of encapsulation of a synthetic long peptide in PLGA nanoparticles: low-burst release is crucial for efficient CD8(+) T cell activation. European Journal of Pharmaceutics and Biopharmaceutics, 83 (3): 338-345, 2013.

[35] Hamdy, S.; Molavi, O.; Ma, Z.; Haddadi, A.;, Alshamsan A.; Gobti, Z.; Elhasi, S.; Samuel, J.; Lavasanifar, A.; Co-delivery of cancer-associated antigen and Toll-like receptor 4 ligand in PLGA nanoparticles induces potent CD8+ T cell-mediated anti-tumor immunity. Vaccine, 26(39):5046-57, 2008.

[36] Butts, C.; Maksymiuk, A; Goss,; Soulieres, D.; Marshall, E.; Cormier, Y.; Ellis, P.M.; Price, A.; Sawhney, R.; Beier, F.; Falk, M.; Murray, N., Updated survival analysis in patients with stage IIIB or IV non-small-cell lung cancer receiving BLP25 liposome vaccine (L-BLP25): phase IIB randomized, multicenter, open-label trial. Journal of Cancer Research and Clinical Oncology, 137 (9): 1337-1342, 2011.

[37] Varypataki, E. M.; Silva, A. L.; Barnier-Quer, C.; Collin, N.; Ossendorp, F.; Jiskoot, W., Synthetic long peptide-based vaccine formulations for induction of cell mediated immunity: A comparative study of cationic liposomes and PLGA nanoparticles. Journal of controlled release, 226: 98-106, 2016.

[38] Li, D.; van Nostrum, C. F.; Mastrobattista, E.; Vermonden, T.; Hennink, W. E., Nanogels for intracellular delivery of biotherapeutics. Journal of Controlled Release, 259: 16-28, 2017.

[39] Jiang, Y.; Chen, J.; Deng, C.; Suuronen, E. J.; Zhong, Z., Click hydrogels, microgels and nanogels: Emerging platforms for drug delivery and tissue engineering. Biomaterials, 35 (18): 4969-4985, 2014.

[40] Zhang, H.; Zhai, Y.; Wang, J.; Zhai, G., New progress and prospects: The application of nanogel in drug delivery. Materials Science & Engineering. C, Materials for Biological Applications, 60, 560-568, 2016.

[41] Dragan, E. S., Design and applications of interpenetrating polymer network hydrogels. A review. Chemical Engineering Journal, 243: 572-590, 2014.

[42] Kordalivand, N.; Li, D.; Beztsinna, N.; Sastre Torano, J.; Mastrobattista, E.; van Nostrum, C. F.; Hennink, W. E.; Vermonden, T., Polyethyleneimine coated nanogels for the intracel-

lular delivery of RNase A for cancer therapy. Chemical Engineering Journal, 340, 32-41, 2018.

[43] Hamidi, M.; Azadi, A.; Rafiei, P., Hydrogel nanoparticles in drug delivery. Advanced Drug Delivery Reviews, 60 (15): 1638-1649:2008.

[44] Raemdonck, K.; Naeye, B.; Buyens, K.; Vandenbroucke, R. E.; Høgset, A.; Demeester, J.; De Smedt, S. C., Biodegradable dextran nanogels for RNA interference: focusing on endosomal escape and intracellular siRNA delivery. Advanced Functional Materials, 19 (9): 1406-1415, 2009.

[45] Vermonden, T.; Censi, R.; Hennink, W. E., Hydrogels for Protein Delivery. Chemical Reviews, 112 (5): 2853-2888, 2012.

[46] Mauri, E.; Cappella, F.; Masi, M.; Rossi, F., PEGylation influences drug delivery from nanogels. Journal of Drug Delivery Science and Technology, 46: 87-92, 2018.

[47] Naeye, B.; Raemdonck, K.; Remaut, K.; Sproat, B.; Demeester, J.; De Smedt, S. C., PEGylation of biodegradable dextran nanogels for siRNA delivery. European Journal of Pharmaceutical Sciences, 2010, 40 (4): 342-351, 2010.

[48] Murphy, E. A.; Majeti, B. K.; Mukthavaram, R.; Acevedo, L. M.; Barnes, L. A.; Cheresh, D. A., Targeted nanogels: a versatile platform for drug delivery to tumors. Molecular Cancer Therapeutics, 10 (6): 972-982, 2011.

[49] Akinc, A.; Battaglia, G., Exploiting endocytosis for nanomedicines, Cold Spring Harbor Perspectives in Biology, 5(11): a016980, 2013.

[50] Sahay, G.; Alakhova, D.Y.; Kabanov, A.V., Endocytosis of nanomedicines, Journal of Controlled Release, 145(3):182-195, 2010.

[51] Li, Y.; Maciel, D.; Rodrigues, J.; Shi, X.; Tomás, H., Biodegradable polymer nanogels for drug/nucleic acid delivery. Chemical Reviews, 115 (16): 8564-8608, 2015.

[52] Wu, H.-Q.; Wang, C.-C., Biodegradable smart nanogels: a new platform for targeting drug delivery and biomedical diagnostics. Langmuir, 32 (25): 6211-6225, 2016.

[53] Molla, M. R.; Marcinko, T.; Prasad, P.; Deming, D.; Garman, S. C.; Thayumanavan, S., Unlocking a caged lysosomal protein from a polymeric nanogel with a pH trigger. Biomacromolecules, 15 (11): 4046-4053, 2014.

[54] Wen, J.; Anderson, S. M.; Du, J.; Yan, M.; Wang, J.; Shen, M.; Lu, Y.; Segura, T., Controlled protein delivery based on enzyme-responsive nanocapsules. Advanced Materials, 23 (39): 4549-4553, 2011.

[55] Meng, F.; Hennink, W. E.; Zhong, Z., Reduction-sensitive polymers and bioconjugates for biomedical applications. Biomaterials, 30 (12): 2180-2198, 2009.

[56] Brulisauer, L.; Gauthier, M. A.; Leroux, J. C., Disulfide-containing parenteral delivery systems and their redox-biological fate. Journal of Controlled Release, 195: 147-154, 2014.

[57] Li, D.; Kordalivand, N.; Fransen, M. F.; Ossendorp, F.; Raemdonck, K.; Vermonden, T.; Hennink, W. E.; van Nostrum, C. F., Cationic nanogels: reduction-sensitive dextran nanogels aimed for intracellular delivery of antigens, Advanced Functional Materials, 25 (20): 2992, 2015.

[58] Jiang, X1.; Wang, X., Cytochrome C-mediated apoptosis, Annual Review of Biochemistry, 73:87-106, 2004.

[59] Biswas, A1.; Joo, KI.; Liu, J.; Zhao, M.; Fan, G.; Wang, P.; Gu, Z.; Tang, Y., Endoprotease-mediated intracellular protein delivery using nanocapsules. ACS Nano, 5(2):1385-1394, 2011.

[60] Li, D.; Sun, F.; Bourajjaj, M.; Chen, Y.; Pieters, E. H.; Chen, J.; van den Dikkenberg, J. B.; Lou, B.; Camps, M. G.; Ossendorp, F.; Hennink, W. E.; Vermonden, T.; van Nostrum, C. F., Strong in vivo antitumor responses induced by an antigen immobilized in nanogels via

reducible bonds. Nanoscale, 8 (47): 19592-19604, 2016.

[61] van Dijk-Wolthuis, W. N. E.; Franssen, O.; Talsma, H.; van Steenbergen, M. J.; Kettenes-van den Bosch, J. J.; Hennink, W. E., Synthesis, characterization, and polymerization of glycidyl methacrylate derivatized dextran. Macromolecules, 28 (18), 6317-6322, 1995.

[62] van Dijk-Wolthuis, W. N. E.; Kettenes-van den Bosch, J. J.; van der Kerk-van Hoof, A.; Hennink, W. E., Reaction of dextran with glycidyl methacrylate: an unexpected trans-esterification. Macromolecules, 30 (11): 3411-3413, 1997.

[63] Winzler, C.; Rovere, P.; Rescigno, M.; Granucci, F.; Penna, G.; Adorini, L.; Zimmermann, V. S.; Davoust, J.; Ricciardi-Castagnoli, P., Maturation stages of mouse dendritic cells in growth factor-dependent long-term cultures. The Journal of Experimental Medicine, 185 (2):317-328, 1997.

[64] Sanderson, S.; Shastri, N., LacZ inducible, antigen/MHC-specific T cell hybrids. International Immunology, 6 (3): 369-376, 1994.

[65] Coin, I.; Beyermann, M.; Bienert, M., Solid-phase peptide synthesis: from standard procedures to the synthesis of difficult sequences. Nature Protocols, 2: 3247-3256, 2007.

[66] Cory, A. H.; Owen, T. C.; Barltrop, J. A.; Cory, J. G., Use of an aqueous soluble tetrazolium/formazan assay for cell growth assays in culture. Cancer Communications, 3 (7): 207-212, 1991.

[67] Sanderson, S.; Shastri, N., LacZ inducible, antigen/MHC-specific T cell hybrids. International Immunology, 6 (3), 369-376, 1994.

[68] Zom, G. G.; Khan, S.; Britten, C. M.; Sommandas, V.; Camps, M. G.; Loof, N. M.; Budden, C. F.; Meeuwenoord, N. J.; Filippov, D. V.; van der Marel, G. A.; Overkleeft, H. S.; Melief, C. J.; Ossendorp, F., Efficient induction of antitumor immunity by synthetic toll-like receptor ligand-peptide conjugates. Cancer Immunology Research, 2 (8): 756-764, 2014.

[69] Komanduri, K. V.; Viswanathan, M. N.; Wieder, E. D.; Schmidt, D. K.; Bredt, B. M.; Jacobson, M. A.; McCune, J. M., Restoration of cytomegalovirus-specific CD4+ T-lymphocyte responses after ganciclovir and highly active antiretroviral therapy in individuals infected with HIV-1. Nature Medicine, 4 (8): 953-956, 1998.

[70] Yadav, M.; Jhunjhunwala, S.; Phung, Q. T.; Lupardus, P.; Tanguay, J.; Bumbaca, S.; Franci, C.; Cheung, T. K.; Fritsche, J.; Weinschenk, T.; Modrusan, Z.; Mellman, I.; Lill, J. R.; Delamarre, L., Predicting immunogenic tumour mutations by combining mass spectrometry and exome sequencing. Nature, 515 (7528): 572-576, 2014.

[71] Foged, C.; Brodin, B.; Frokjaer, S.; Sundblad, A., Particle size and surface charge affect particle uptake by human dendritic cells in an in vitro model. International Journal of Pharmaceutics, 298(2):315-322, 2005.

[72] Slawek, A.; Maj, T.; Chelmonska-Soyta, A., CD40, CD80, and CD86 costimulatory molecules are differentially expressed on murine splenic antigen-presenting cells during the pre-implantation period of pregnancy, and they modulate regulatory T-cell abundance, peripheral cytokine response, and pregnancy outcome. American Journal of Reproductive Immunology, 70 (2): 116-126, 2013.

[73] Bancos, S.; Tyner, K. M.; Weaver, J. L., Immunotoxicity testing for drug–nanoparticle conjugates: regulatory considerations. In Handbook of Immunological Properties of Engineered Nanomaterials, McNeil, S. E., Ed. World Scientific Publishing Ltd.: Singapore, pp 671-685.

[74] Sakaguchi, S.; Yamaguchi, T.; Nomura, T.; Ono, M., Regulatory T cells and immune tolerance. Cell, 133 (5): 775-787, 2008.

1

2

3

4

5

6

7

8

&